Geochemistry Geophysics Geosystems G3
AN ELECTRONIC JOURNAL OF THE EARTH SCIENCES
Published by AGU and the Geochemical Society

Article
Volume 7, Number 1
XX Month 2006
XXXXXX, doi:10.1029/2005GC001002
ISSN: 1525-2027

Long-term volumetric eruption rates and magma budgets

Scott M. White
Department of Geological Sciences, University of South Carolina, 700 Sumter Street, Columbia, South Carolina 29208, USA (swhite@geol.sc.edu)

Joy A. Crisp
Jet Propulsion Laboratory, California Institute of Technology, Pasadena, California 91109, USA (joy.a.crisp@jpl.nasa.gov)

Frank J. Spera
Department of Earth Science, University of California, Santa Barbara, Santa Barbara, California 93106, USA (spera@geol.ucsb.edu)

[1] A global compilation of 170 time-averaged volumetric volcanic output rates (Q_e) is evaluated in terms of composition and petrotectonic setting to advance the understanding of long-term rates of magma generation and eruption on Earth. Repose periods between successive eruptions at a given site and intrusive:extrusive ratios were compiled for selected volcanic centers where long-term (>10^4 years) data were available. More silicic compositions, rhyolites and andesites, have a more limited range of eruption rates than basalts. Even when high Q_e values contributed by flood basalts ($9 \pm 2 \times 10^{-1}$ km^3/yr) are removed, there is a trend in decreasing average Q_e with lava composition from basaltic eruptions ($2.6 \pm 1.0 \times 10^{-2}$ km^3/yr) to andesites ($2.3 \pm 0.8 \times 10^{-3}$ km^3/yr) and rhyolites ($4.0 \pm 1.4 \times 10^{-3}$ km^3/yr). This trend is also seen in the difference between oceanic and continental settings, as eruptions on oceanic crust tend to be predominately basaltic. All of the volcanoes occurring in oceanic settings fail to have statistically different mean Q_e and have an overall average of $2.8 \pm 0.4 \times 10^{-2}$ km^3/yr, excluding flood basalts. Likewise, all of the volcanoes on continental crust also fail to have statistically different mean Q_e and have an overall average of $4.4 \pm 0.8 \times 10^{-3}$ km^3/yr. Flood basalts also form a distinctive class with an average Q_e nearly two orders of magnitude higher than any other class. However, we have found no systematic evidence linking increased intrusive:extrusive ratios with lower volcanic rates. A simple heat balance analysis suggests that the preponderance of volcanic systems must be open magmatic systems with respect to heat and matter transport in order to maintain eruptible magma at shallow depth throughout the observed lifetime of the volcano. The empirical upper limit of $\sim 10^{-2}$ km^3/yr for magma eruption rate in systems with relatively high intrusive:extrusive ratios may be a consequence of the fundamental parameters governing rates of melt generation (e.g., subsolidus isentropic decompression, hydration due to slab dehydration and heat transfer between underplated magma and the overlying crust) in the Earth.

Components: XXX words, 6 figures, 4 tables, 1 dataset.

Keywords: volcanism; magma budget; rates; volcanic repose.

Index Terms: 8145 Tectonophysics: Physics of magma and magma bodies; 8411 Volcanology: Thermodynamics (0766, 1011, 3611); 8499 Volcanology: General or miscellaneous.

Received 18 April 2005; **Revised** 3 November 2005; **Accepted** 21 December 2005; **Published** XX Month 2006.

White, S. M., J. A. Crisp, and F. A. Spera (2006), Long-term volumetric eruption rates and magma budgets, *Geochem. Geophys. Geosyst.*, *7*, XXXXXX, doi:10.1029/2005GC001002.

1. Introduction

[2] Despite the significant impact of volcanic systems on climate, geochemical cycles, geothermal resources and the evolution and heat budget of the crust, surprisingly little is known regarding the systematics of long-term rates of magma generation and eruption on Earth. Global rates of magma generation provide insight regarding the planetary-scale energy budget and thermal evolution of the Earth. Rates of magma generation and eruption are key factors affecting the petrological and geochemical evolution of magma bodies as well as eruptive styles due to the intrinsic coupling between magma recharge, fractional crystallization, wall rock assimilation and melt volatile saturation [*Shaw*, 1985; *Spera et al.*, 1982]. Volcanoes and formation of intrusive bodies such as sill complexes have been suggested to play a role in global climate change [*Svensen et al.*, 2004] and perhaps even trigger biotic extinctions. In addition, global rates of magmatism may have important implications for seismic energy release [*Shaw*, 1980] and the magnetic geodynamo by modulating heat transfer from the core-mantle boundary and the concomitant development of deep mantle plumes [*Olson*, 1994]. Rates of magmatism on Earth are also used in planetary research as analogues to constrain magmatic and thermal models. In summary, there is an exhaustive set of reasons for developing systematic knowledge regarding the rates of magmatism on Earth including the effects of magma composition and petrotectonic environment on volumetric rates.

[3] One of the key factors in understanding magmatism is a quantitative evaluation of the extent to which magmatic systems operate as open or closed systems. These alternatives have significantly different implications for magma evolution. However, the openness of magmatic systems is difficult to determine since there is no unambiguous way to track magma transport from the generation and segregation through the crust to volcanic output. On balance, many magma systems are thought to be open systems in that they receive additional inputs of heat and mass during magmatic evolution [*Davidson et al.*, 1988; *Fowler et al.*, 2004; *Gamble et al.*, 1999; *Hildreth et al.*, 1986; *Petford and Gallagher*, 2001]. Closed magmatic systems which exchange heat but little material with their surroundings (i.e., neither assimilation nor recharge is important) may be rather uncommon. What is more likely is that specific systems may behave as closed systems for restricted portions of their history [e.g., *Singer et al.*, 1992; *Zielinski and Frey*, 1970]. It is important to note, however, for the olivine basalt-trachyte series at Gough Island where fractional crystallization appears dominant, Pb and Sr isotopic data indicates that assimilation of hydrothermally altered country rock and/or recharge of isotopically distinct magma has taken place [*Oversby and Gast*, 1970].

[4] In this paper, time-averaged volcanic output for periods $>10^3$ years are evaluated. Volcanic output rates for individual eruptions may vary wildly about some norm, but evidently settle to a representative “average” value when time windows on the order of 10 times the average interval of eruptions are considered [*Wadge*, 1982]. *Crisp* [1984] conducted a similar study of magmatic rates published between 1962 and 1982 and established some basic relationships between volcanic output and associated factors such as crustal thickness, magma composition, and petrotectonic setting. This work updates and extends that earlier compilation with 98 newly published volcanic rates and volumes from 1982–2004 for a total of 170 estimates (see auxiliary material[1] Tables S1 and S2). We also endeavor to establish some scaling relationships based primarily on the compilation and some simple energy budget considerations with the goal of discovering possible systematic trends in the data.

2. Sources and Quality of the Data

[5] The data presented here are volumetric volcanic or intrusive rates published from 1962–2005, including data from the compilation by *Crisp* [1984] of rates published from 1962–1982 where these data have not been superseded by more recent studies. We have also reviewed the rate data presented by *Crisp* [1984] and corrected or removed several references as appropriate. Thus the data presented here is a completely updated compilation of volumetric rates of eruption.

[6] Most volcanoes have cycles of intense activity followed by repose. Comparing volcanic systems at different stages in their eruptive cycles can lead to erroneous conclusions, if the duration of activity is not long enough to average the full range of eruptive behavior over the lifetime of the volcano. The duration needed depends upon the individual volcano; longer periods are generally required for

[1] Auxiliary material is available at ftp://ftp.agu.org/apend/gc/2005GC001002.

volcanic centers erupting more compositionally evolved magma due to lower eruption recurrence interval. Thus a period of $\sim 10^3$ years may be a long time for a basaltic shield volcano (e.g., Kilauea, Hawaii) but captures only an insignificant fraction of one eruptive cycle at a rhyolitic caldera (e.g., Yellowstone, USA). Only long-term rates are considered in this study although this reduces the available data considerably. We have culled the data to include primarily those estimates over 10^4 years or longer, but have selected a few volcanic centers with shorter durations where the shorter time interval did not compromise the data quality (e.g., capturing several eruptive cycles, smaller volcanic centers, or similar reasons) in our judgment.

[7] Tables 1 and 2 show volcanic output rates for primarily mafic and silicic systems respectively. Output rates for volcanic systems (Q_e) are determined by dividing volcanic output volume by the duration of the activity. For longer durations activity may not have been continuous. By use of density for different compositions [*Spera*, 2000] we can convert volume rate (Q_e) to mass rate, which is probably the more fundamental parameter. Since density varies only slightly (basalt is $\sim$15% denser than rhyolite at the same temperature and pressure) compared to the uncertainty in the data and the original data is all reported in terms of volume, we use Q_e exclusively in the rest of this study although mass rates are also given in Tables 1 and 2. Within each table, the rate estimates encompassing large areas, such as entire arcs or extensive volcanic fields, is presented separately from rates for individual volcanoes or smaller fields of vents. To remove ambiguity from the decision, a cutoff of 10^4 km^2 was used to separate global data sets, typically involving compilations of several volcanoes themselves, from local data sets focused on individual volcanoes with a more constrained study area. However, we find that rates for entire arcs/fields when presented as km^3/yr per 100 km are similar to those for individual volcanoes (Figure 1).

[8] A large amount of uncertainty is associated with inferring volcanic rates from unobserved eruptions. In the tables, a "Notes" field contains information about the methods used to derive the estimates and uncertainties that were available in the original literature, but in many cases no formal uncertainties were reported. Generally the rates reported here should be taken as order-of-magnitude estimates although in some cases the uncertainties may be as small as a factor of two. The extrusive rate often depends on the duration considered; therefore data for one volcanic center measured over different durations are included in Tables 1 and 2. The period of volcanism may also be important since eruptions from further in the past may have experienced more erosion, partial burial, or be more difficult to accurately date.

[9] Sources of error reported in the original publications, as well as most unquantified unreported error, mainly arise from estimating (1) the thickness of the volcanic deposits, (2) the age of lavas, or (3) amount of erosion. Less significant potential sources of error are uncertainty in the conversion from volume to dense rock equivalent (DRE) volume, and uncertainty in the area covered by deposits. One may attribute some of the variance in rates to error introduced by comparing volcanic systems at different scales. For example, the volcanic output rate over continuous lengths of oceanic arcs and ridges is expected to be higher than small individual volcanoes. The arcs and ridges are divided into unit volcano lengths of 100 km based on the spacing of volcanoes in arcs [*de Bremond d'Ars et al.*, 1995]. Petrologic and tectonic factors are also reported for each volcanic system where data are available include lithic type or bulk wt% SiO_2 of erupted magma, and petrotectonic setting. Rock names are given for the dominant magma type associated with each area simplified in one of the following categories: basalt, basaltic andesite, andesite, rhyolite. The mode wt% SiO_2 reported here is the mode of erupted products by volume reported within the given period for that volcanic system. Petrotectonic setting groups the systems into six categories based on crustal type, oceanic or continental, and association with a plate boundary type; convergent, divergent, or intraplate.

3. Volcanic Rates and Regimes

3.1. Rates of Eruption

[10] Eruption rates are examined on the basis of dominant lithology and petrotectonic setting. Rock type affects many factors related to flow behavior such as viscosity, temperature, and pre-eruptive volatile content. Thus it may be an important control on eruption rate. Petrotectonic setting most strongly reflects the magma generation process, but is also a way to qualitatively look at the effects of crustal thickness.

[11] The effect of magma composition on eruption rate is assessed by broadly grouping the lavas from a volcanic area into one of four categories based on the dominant SiO_2 of the reported rock composi-

t1.1 **Table 1 (Representative Sample).** Rates and Volumes of Basaltic Volcanism [The full Table 1 is available in the HTML version of this article at http://www.g-cubed.org]

	Location (Volcano Name)	Duration, Myr	Extrusive Volume, km^3	Volume Extrusion Rate Q_e, $km^3\ yr^{-1}$	Mass Extrusion Rate, $kg\ yr^{-1}$	Bulk SiO_2	Petrotectonic Setting	Notes	References
t1.2									
t1.3	*Area < $10^4 km^2$ (Individual Volcanoes/Small Volcanic Fields)*								
t1.4	Ascension	1.500	90	6.00E−05	1.49E+09	48	oceanic hot spot	Rough estimate of volumes from topography; rates constrained by a few K-Ar dates since 1.5 Ma.	*Gerlach* [1990], *Nielson and Sibbett* [1996]
t1.5	Auckland, New Zealand	0.140	2	1.07E−05	2.89E+07	B	Continental volcanic field	Volume calculated from thickness and areal extent based on field mapping and boreholes for 49 volcanic centers and adjusted to DRE volume. Active for last 140 kyr based on K-Ar, thermoluminescence, and ^{14}C dates.	*Allen and Smith* [1994]
t1.6	Bouvet	0.700	28	4.00E−05	4.59E+08	48	oceanic hot spot	Very rough estimate of volume from island topography; active for the past 0.7 Myr.	*Gerlach* [1990]
t1.7	Camargo, Mexico	4.64	120	2.6E−05	7.02E+07	B	Continental volcanic field	Constraints from K-Ar dates from 4.73 ± 0.04 Ma to 0.09 ± 0.04 Ma. Volume based on an area of 3000 km^2 and average thickness of 40 m	*Aranda-Gomez et al.* [2003]
t1.8	La Palma, Canary Islands	0.123	125	1.0E−03	2.70E+09	48	oceanic hot spot	Detailed field observations, mapping, and $^{39}Ar/^{40}Ar$ dating of uneroded Cumbre Viejo indicate activity since 123 ± 3 ka.	*Carracedo et al.* [1999], *Guillou et al.* [1998]
t1.9	Santo Antao, Cape Verdes	1.750	68	4.00E−05	1.08E+08	48	oceanic hot spot	Rates from main shield-building stage Cha de Morte volcanics deposited between 2.93 ± 0.03 and 1.18 ± 0.01 Ma ($^{39}Ar/^{40}Ar$ ages) and field mapping.	*Plesner et al.* [2002]
t1.10	Coso, CA	1.500	24.3	1.60E−05	5.40E+12	57	continental volcanic field	Field mapping estimate of 23–25.5 km^3 erupted between 4.02 ± 0.06 and 2.52 ± 0.05 Ma (K-Ar ages).	*Duffield et al.* [1980]

t2.1 **Table 2 (Representative Sample).** Rates and Volumes of Silicic Volcanism [The full Table 2 is available in the HTML version of this article at http://www.g-cubed.org]

	Location	Duration, Myr	Extrusive Volume, km^3	Volume Extrusion Rate Q_e, $km^3\ yr^{-1}$	Mass Extrusion Rate, $kg\ yr^{-1}$	SiO_2 Wt%	Petrotectonic Setting	Notes	References
t2.2									
t2.3	*Area < $10^4 km^2$ (Individual Volcanoes/Small Volcanic Fields)*								
t2.4	Alban Hills, Italy	0.561	290	5.2E−04	*1.33E+09*	A	Continental arc	Geologic map. Some ages from thermoluminescence. Period of eruptions 580 ka to 19 ka. Not corrected for DRE. Unknown amount of erosion.	*Chiarabba et al.* [1997]
t2.5	Asama	0.030	37	1.20E−03	8.61E+08	A	oceanic arc	37 ± 7 km^3 erupted over past 0.03 Myr	*Crisp* [1984]
t2.6	Avachinsky, USSR	0.060	100	1.70E−05	1.62E+08	BA	continental arc	Rough estimate excluding ejecta beyond cone.	*Crisp* [1984]
t2.7	Ceboruco-San Pedro	0.8	80.5	8.05E−5	*2.05E+08*	A	continental arc	Volume determinations 80.5 ± 3.5 km^3 from field mapping, digital topography, and orthophotos. Only minor erosion. Age from numerous $^{40}Ar/^{39}Ar$ dates.	*Frey et al.* [2004]
t2.8	Ceboruco-San Pedro	0.1	60.4	6.04E−4	*1.54E+09*	A	continental arc	Volume determinations from field mapping, digital topography, and orthophotos. Only minor erosion. Age from numerous $^{40}Ar/^{39}Ar$ dates.	*Frey et al.* [2004]
t2.9	Clear Lake, California	2.050	73	3.50E−05	2.81E+09	64	Continental Volcanic Field	For period from 2.06–0.01 Ma. Volume includes estimate of eroded material.	*Crisp* [1984]
t2.10	Coso, California	0.4	2.4	5.7E−06	1.34E+07	R	Continental Volcanic Field	Geologic mapping estimate of 0.9 km^3 of basalt and 1.5 km^3 of rhyolite erupted over past 0.4 Myr based on K-Ar ages.	*Bacon* [1982]
t2.11	Davis Mountains, Texas	1.5	1525	1.0E−03	2.35E+09	R	Continental Volcanic Field	Detailed field mapping and $^{40}Ar/^{39}Ar$ ages from 36.8 to 35.3 Ma. No DRE correction applied, as deposits have low porosity. The actual total volume may be as high as 2135 km^3, if buried lava flows over full extent of area suggested.	*Henry et al.* [1994]
t2.12	Fuji	0.011	88	8.00E−03	4.59E+08	BA	oceanic arc	Volume estimated from detailed field mapping for eruptions over past 11 kyr (tephrachronology)	*Togashi et al.* [1991]

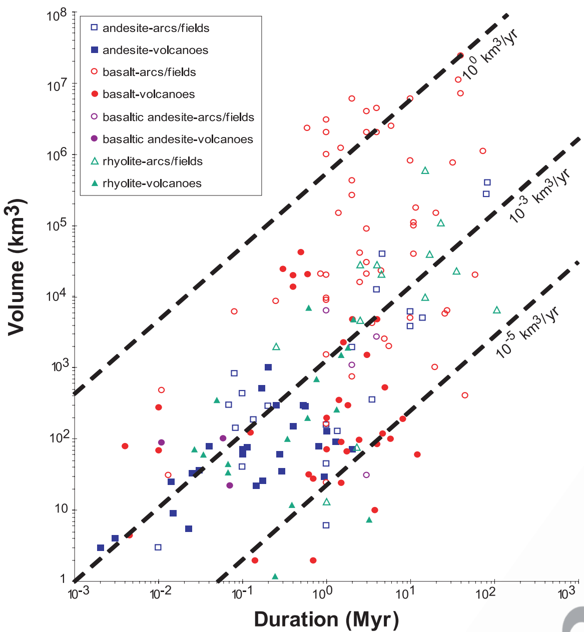

Figure 1. Volumes and volcanism durations for locations in Tables 1 and 2 (see also auxiliary material Tables S1 and S2). The diagonal lines represent constant rates of volcanic output. The points are coded by color and shape to indicate lava composition by SiO_2 content. Open symbols represent rates for arc and large areas ($>10^4$ km^2), and solid symbols represent individual volcanoes and small volcanic fields ($<10^4$ km^2).

tions: basalt, basaltic andesite, andesite, or rhyolite. Many important physical properties of lava are a function of SiO_2 content, as well as being easy to measure and widely reported, making this a useful tool for first-order comparison of volcanoes. The rock type dominant in the area is assigned as the rock type to represent the entire area. For example, Yellowstone is assigned as rhyolite on the basis of its repeated large caldera-forming eruptions even though a small amount of basalt leaks out between large-volume paroxysmal rhyolite eruptions. Where bimodal volcanism is equally balanced by volume or a change in rock type has occurred at some point in the eruptive history of the volcanic system, the basaltic (Table 1) and silicic (Table 2) volumes and rates of eruption are reported separately. For example, recent Kamchatka eruptions are split into andesites (Table 2) and basalts (Table 1).

[12] Basalts exhibit a wider range of eruption rates than other rock types, ranging from $<10^{-5}$ km^3/yr to >1 km^3/yr (Figure 1). Basaltic systems in general show both short-term and long-term changes in eruption rates especially in long-lived systems (e.g., Hawaii [*Dvorak and Dzurisin*, 1993; *Vidal and Bonneville*, 2004]). More-silicic rock types, the rhyolites and andesites, have a more limited range of eruption rates than basalts. Long-term rates for silicic eruptions range from $<10^{-5}$ km^3/kyr to 10^{-2} km^3/yr (Table 2 and Figure 1). Among the major rock type groups we have used here, the mean and variance of Q_e decreases as the amount of silica increases. In Figure 1, this trend is apparent as the basalts form a wide field of values whose mean is 10^{-2} km^3/yr while andesites and rhyolites form a much narrower band of values around 10^{-3} km^3/yr. The flood basalts form a small cluster of values above 1 km^3/yr on Figure 1, outside of a more uniform field of values for all compositions, and seem to form a distinct group. Therefore flood basalts were not considered with the rest of the basalt rates when comparing to other compositions to avoid skewing the results. With flood basalts removed, basaltic eruptions still have an order-of-magnitude higher average rate ($2.6 \pm 1.0 \times 10^{-2}$ km^3/yr) than basaltic andesites, andesites and rhyolites. Average rates for andesites ($2.3 \pm 0.8 \times 10^{-3}$ km^3/yr) and rhyolites ($4.0 \pm 1.4 \times 10^{-3}$ km^3/yr) are also significantly different, although not as distinct as the difference between basalts and these two groups.

[13] The effect of petrotectonic setting on eruption rate is assessed by grouping the volcanoes by the main differences in magma genesis based on plate tectonic theory. In contrast to lithology, petrotectonic setting lends itself to grouping into categories (Figure 2). Volcanoes at convergent plate boundaries are arcs, divergent plate boundaries are rifts or spreading ridges, and intraplate volcanoes are so-called hot spots. Also included is a separate designation of volcanic fields (continental volcanic fields) for areas characterized by areally distributed volcanism of primarily small (<1 km^3), monogenetic cones. These fields tend to occur in regions that are difficult to classify by traditional plate tectonic theory such as slab windows (e.g., Clear Lake, CA) or continental extension (e.g., Lunar Crater, NV). In order to also assess the role of crustal thickness/composition, the petrotectonic settings are further subdivided into volcanoes erupting through continental or oceanic crust. The exceptions are oceanic plateaux, the flood basalt equivalent for oceanic crust. Reliable data are so sparse for plateaux that we have grouped oceanic and continental flood basalts in Figure 2.

[14] Flood basalts have the highest single Q_e value and mean Q_e of any volcanic system on Earth (Figure 2). In this respect, flood basalts form an exceptional group unlike the other forms of terrestrial volcanism. In contrast, the continental volcanic fields have the lowest single and mean Q_e of

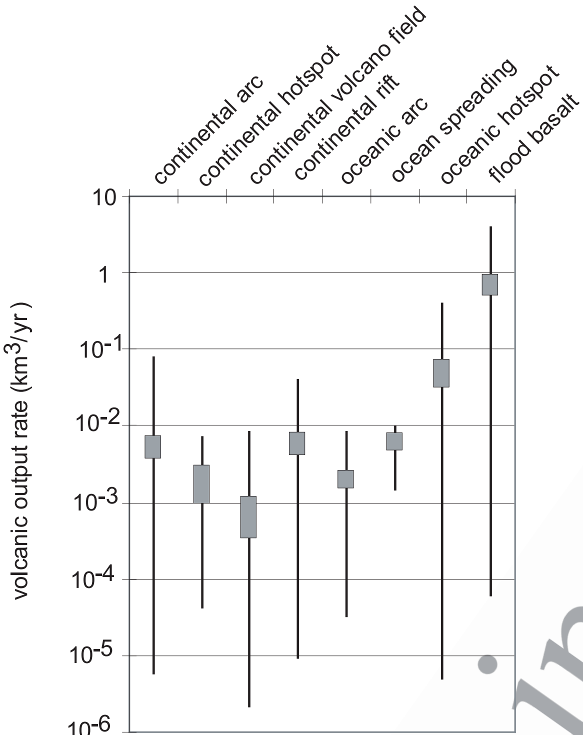

Figure 2. Volcanic rates grouped by petrotectonic setting for all locations in Tables 1 and 2. Shaded boxes represent the range of one standard deviation from the mean rate. The black bars show the minimum and maximum rates for each setting. For all settings, mean Q_e is skewed toward high values, which may imply a natural upper limit set by magma generation but no lower limit.

any group. A very wide range of eruption rates have been reported for oceanic hot spots that overlaps significantly with oceanic arcs and ocean spreading ridges. Although the mean Q_e appears higher for oceanic hot spots than other classes of oceanic volcanism, the two-tailed t-test indicates that Q_e for all groups of oceanic volcanism are not statistically different. When grouped by petrotectonic setting, Q_e from continental areas tend to be lower on average than for oceanic areas, however the range of output rates for any one setting overlaps all other settings (Figure 2). *Crisp* [1984] noted a similar pattern of higher eruption rates in oceanic settings although found no specific value of crustal thickness that acted as a filter threshold. All of the volcanoes occurring in oceanic settings fail to have statistically different mean Q_e and have an overall average of $2.8 \pm 0.5 \times 10^{-2}$ km^3/yr. Likewise, all of the volcanoes on continental crust also fail to have statistically different mean Q_e and have an overall average of $4.4 \pm 0.8 \times 10^{-3}$ km^3/yr, excluding flood basalts. A two-tailed t-test for means indicates that oceanic and continental Q_e are statistically different. This implies that crustal thickness, as the overarching contrast between oceanic and continental lithosphere, exerts some control on volcanic rates. Flood basalts also form a distinctive class of volcanism with an average Q_e ($9 \pm 2 \times 10^{-1}$ km^3/yr) two orders of magnitude larger than the range of any other class (Figure 2).

3.2. Intrusive:Extrusive Ratios

[15] The average and range of intrusive:extrusive (I:E) volume ratios for different petrotectonic settings are useful in estimating hidden intrusive volumes at other locations and perhaps on other planets [*Greeley and Schneid*, 1991]. However, I:E ratios are difficult to estimate and rarely published because the plutonic rocks are either buried or the volcanic rocks are eroded, or the relationship between the volcanic and plutonic rocks is uncertain. Seismic, geodetic, and electromagnetic techniques can reveal the dimensions of molten or partially molten regions under a volcano. Likewise, the sulfur output by magma degassing can be used to estimate the volume of the cooling magma [*Allard*, 1997]. However, the size of the molten magma reservoir at one time in a longer history may not be a good indicator of the total intrusive volume. Likewise, broad constraints on intrusive volume based on petrologic modeling of the fractional crystallization of a parent basalt are not considered because they will always calculate lower bound on intrusive volume, because such calculations based on extrusive rocks cannot account for strictly intrusive events. Better estimates of total intrusive volume can sometimes be obtained by seismic or gravity measurements of buried plutons. Another way to determine I:E ratios is to compare geographically related volcanic and plutonic sequences. Three such determinations were made in this compilation for the Andes, the Bushveld Complex, and the Challis Volcanic Field-Casto Pluton. However, in each of these cases it is uncertain how well linked extrusive and intrusive rocks are in fact. Despite this uncertainty, we proceed with an analysis if for no other reason than to highlight that this issue has received so little attention.

[16] Previous studies have reported a wide range of I:E ratios from 1:1 to 16:1 [*Crisp*, 1984; *Shaw et al.*, 1980; *Wadge*, 1980]. *Shaw* [1980] hypothesized that the I:E ratio would be higher where crustal thickness is greater, up to 10:1. This makes sense since magma traveling greater path lengths through thicker continental crust has longer to cool

Geochemistry Geophysics Geosystems G3

t3.1 **Table 3.** Intrusive:Extrusive Ratios

t3.2	Volcano	Intrusive	Extrusive	Ratio	Method	References
t3.3	Aleutians	1073–1738 km^3/km	627–985 km^3/km	1:1–3:1[a]	Seismic and crystallization of Hidden Bay Pluton and related extrusives	*Kay and Kay* [1985]
t3.4	Bushveld-Rooiberg, South Africa	1×10^6 km^3	3×10^5 km^3	3:1	Stratigraphic mapping. Cr and incompatible trace element analyses indicate that the total magma volume intruded was approximately 1×10^6 km^3.	*Cawthorn and Walraven* [1998], *Schweitzer et al.* [1997], *Twist and French* [1983]
t3.5	Central Andes, Peru	$9–29 \times 10^4$ km^3	2.25×10^4 km^3	3:1–12:1	Extrusive from geologic mapping. Intrusive from mapping and gravity.	*Francis and Hawkesworth* [1994], *Haederle and Atherton* [2002]
t3.6	Challis Volcanic Field, Idaho	3.5×10^3 km^3	$4 \times 10^3 - 2.8 \times 10^4$ km^3	>1:1–8:1	Very uncertain; field and stratigraphic mapping; extrusive converted to DRE using 75% porosity; total plutonic thickness unknown	*Criss et al.* [1984]
t3.7	Coso Volcanic field, California	2.8 km^3/Myr (basalt) 5.4 km^3/Myr (rhyolite)	570 km^3/Myr	1:200[a] 1:100[a]	Extrusive from geologic mapping for the past 0.4 Myr; intrusive rate based on current heat flow and estimates of local tectonic extension.	*Bacon* [1983]
t3.8	East Pacific Rise	7 km	0.5–0.8 km	5:1–8:1	Seismic; stratigraphic mapping.	*Detrick et al.* [1993], *Harding et al.* [1993], *Karson* [2002]
t3.9	Etna, Italy (1 Ma)	3×10^2 km^3	1×10^2 km^3	3:1	Seismic (estimate for ~0.1 Ma).	*Allard* [1997], *Hirn et al.* [1991]
t3.10	Italy (since 1975)	0.6 km^3	5.9 km^3	10:1	SO_2 flux 1975–1995 AD.	
t3.11	Hawaiian-Emperor Seamount Chain	5.9×10^6 km^3	1.1×10^6 km^3	6:1[a]	Extrusive from topographic maps; intrusive from flexural models and seismic, averaged over the past 74 Myr.	*Bargar and Jackson* [1974], *Vidal and Bonneville* [2004]
t3.12	Iceland	5 km	20–40 km	4:1–8:1	Seismic.	*Bjarnason et al.* [1993], *Darbyshire et al.* [1998], *Menke et al.* [1998], *Staples et al.* [1997]
t3.13	Kerguelen Archipelago	9.9×10^4 km^3	2.75×10^6 km^3	28:1[a]	Seismic.	*Nicolaysen et al.* [2000]
t3.14	Kilauea, Hawaii	9×10^{-2} km^3/yr	5×10^{-2} km^3/yr	2:1	Drill hole stratigraphy; ground deformation; geologic mapping.	*Dvorak and Dzurisin* [1993], *Quane et al.* [2000]
t3.15	Long Valley, California	7.6×10^3 km^3	7.5×10^2 km^3	10:1	Rough estimate from seismic tomography, stratigraphic mapping, drill holes, and gravity.	*Hildreth* [2004], *McConnell et al.* [1995], *Weiland et al.* [1995]
t3.16	Marquesas Islands	6.2×10^5 km^3	3.3×10^5 km^3	2:1[a]	Seismic.	*Caress et al.* [1995]
t3.17	Mauna Loa, Hawaii	8×10^1 km^3	$1.1–2.4 \times 10^2$ km^3	>1:1–3:1	Stratigraphic mapping, for the 1877–1950 time period.	*Klein* [1982], *Lipman* [1995]
t3.18	Mid-Atlantic Ridge	5.5–7 km	0.5–1.5 km	5:1–10:1	Seismic.	*Hooft et al.* [2000]
t3.19	Miyake, Japan	4 km^3	1.5×10^{-1} km^3	3:1	Geodetic modeling; SO_2 emissions.	*Kumagai et al.* [2001]
t3.20	Mull Volcano, Scotland	1.3×10^4 km^3	7.6×10^3 km^3	2:1	Stratigraphic mapping.	*Walker* [1993]
t3.21	Ninetyeast Ridge	7–8 km	3–4 km	2:1	Seismic.	*Grevemeyer et al.* [2001], *Nicolaysen et al.* [2000]

Table 3. (continued)

Volcano	Intrusive	Extrusive	Ratio	Method	References
Pinatubo, Philippines	60–125 km^3	3.7–5.3 km^3	11:1–34:1	Seismic, stratigraphic mapping.	*Mori et al.* [1996], *Wolfe and Hoblitt* [1996]
San Francisco Mountain, Arizona	94 km^3	500 km^3	6:1	Geologic mapping, estimated amount of eroded material included, and seismic low-velocity body with a volume of 300–700 km^3.	*Tanaka et al.* [1986]
Twin Peaks, Utah	290–430 km^3	40–43 km^3	5:1–9:1	Geologic mapping, gravity and thermal modeling.	*Carrier and Chapman* [1981], *Crecraft et al.* [1981], *Evans et al.* [1980]
Yellowstone	6.5 × 10^3 km^3	1.89 × 10^4 km^3	3:1	Seismic; stratigraphic mapping.	*Christiansen and Blank* [1972], *Clawson et al.* [1989], *Miller and Smith* [1999]

[a] Values that include crustal underplating.

and dissipate energy. In addition, mean crustal densities are closer to typical magma densities compared to the mantle (i.e., positive buoyancy forces are likely smaller for magma in the crust compared to magma in the mantle). Subsequently, *Wadge* [1982] made the argument based on steady state volcanic rates and indirect calculations of intrusive volume that less evolved systems have I:E ratios as low as 1:1.5 for basaltic shields on oceanic crust and up to 1:10 for rhyolite calderas on continental crust. *Crisp* [1984] presented 14 ratios but did not find any strong connection between magma composition and I:E ratio.

[17] The I:E ratios in this compilation encompass a wide range of values but fails to show any systematic variations with eruptive style, volcanic setting, or total volume (Table 3). While some well-known basaltic shields do have I:E ratios of 1:1 to 2:1, the oceanic ridges have considerably higher ratios of at least 5:1. The range of estimates goes as high as 34:1 at Mount Pinatubo, and 200:1 for the Coso Volcanic Field. Conversely, the I:E ratios at calderas may be much lower than 10:1. Yellowstone has a fairly well constrained I:E ratio of 3:1. Continental magma systems that have had detailed geophysical investigations tend to have magma chamber volume estimates comparable to the total erupted volume, as noted by *Marsh* [1989]. A ratio of 5:1 could be viewed as common to most magmatic systems when the considerable uncertainty is considered. Ratios higher than 10:1 are uncommon in our data set. When volume of magma involved in crustal "underplating" or magmatic addition to the lower crust is also counted, much higher ratios of intrusive:extrusive activity sometimes result (Ninetyeast Ridge [*Frey et al.*, 2000], Coso [*Bacon*, 1983]) but other times do not (Aleutians [*Kay and Kay*, 1985], Marquesas [*Caress et al.*, 1995]).

3.3. Repose Time Between Volcanic Events

[18] A major discriminant in the behavior of volcanic systems is their frequency of eruptions through time. Most basaltic volcanoes erupt small volumes of lava frequently whereas continental calderas erupt great volumes of silicic magma infrequently. At Hekla, *Thorarinsson and Sigvaldason* [1972] noted a positive relationship between repose length and the silica content of the initial lavas erupted following the repose. Data from 17 volcanic centers in Table 4 selected to span a wide range of SiO_2 content define an exponential relationship between repose time and SiO_2 content in the lava (Figure 3). The volcanic centers in Table 4 were chosen to span

Table 4. Repose Times at Selected Volcanic Centers

Volcano	Repose Time Avg, years	Repose Min, years	Repose Max, years	Number of Reposes in Record	wt% SiO2 min	wt% SiO2 max	References	Notes
Colima	80	48	138	3	56	61	*Luhr and Carmichael* [1980]	Four cycles of activity ending with ash flow eruptions since 1576 AD.
Etna	4	0.1	100	70	47	50	*Tanguy* [1979], *Wadge* [1977]	Constrained by historical records from 1536 to 2001 AD.
Fogo, Cape Verde	20	1	94	27	40	42	*Doucelance et al.* [2003], *Trusdell et al.* [1995]	Constrained by historical records from 1500 to 1995 AD.
Fuego	100	10	150	60	49	55	*Martin and Rose* [1981]	Constrained by historical records since 1500 AD; eruptions occur in clusters of activity.
Izu-Oshima	68	13	190	23	53	57	*Koyama and Hayakawa* [1996]	Detailed syncaldera and postcaldera eruptive history from tephra and loess stratigraphy; reposes since caldera formation.
Katla	46	13	80	20	46	50	*Larsen* [2000]	Last 11 centuries; constrained by historical records.
Kilauea	0.8	0.1	10	46	48	50	*Klein* [1982]	Constrained by historical records from 1918 to 1979 AD.
Mauna Loa	5	0.1	20	34	48	50	*Klein* [1982]	Constrained by historical records from 1843 to 1984 AD.
Mt Adams	150000	50000	320000	3	57	64	*Hildreth and Fierstein* [1997], *Hildreth and Lanphere* [1994]	Major cone building episodes since 500 ka.
Mt St Helens	8600	5000	15000	6	63	67	*Doukas* [1990], *Mullineaux* [1996]	From 40 ka to present, major eruptive cycles only.
Ruapehu	30000	10000	60000	5	55	65	*Gamble et al.* [2003]	Constrained by $^{40}Ar/^{39}Ar$ ages.
Santorini	30000	17000	40000	12	58	71	*Druitt et al.* [1999]	For major explosive volcanism since 360 ka. Both $^{40}Ar/^{39}Ar$ and K-Ar ages for older units, radiocarbon ages for younger.
Taupo	2000	20	6000	28	72	76	*Sutton et al.* [2000]	Post-Oruanui eruptions from 26.5 ka to present.
Toba	375000	340000	430000	3	68	77	*Chesner and Rose* [1991]	Reposes between tuff-forming eruptions since 0.8 Ma.
Valles	335000	320000	350000	3	69	75	*Doell et al.* [1968], *Heiken et al.* [1990]	Reposes based on eruption of Bandelier and pre-Bandelier tuff, and collapse of Toledo and Valles calderas.
Yatsugatake	32000	10000	85000	5	53	63	*Kaneoka et al.* [1980], *Oishi and Suzuki* [2004]	Plinian eruptions since 0.2 Ma. Tephrochonology and radiocarbon ages.
Yellowstone	700000	600000	800000	3	75	79	*Christiansen* [2001]	Considers major tuff-forming eruptions.

a range of SiO_2 compositions for sequences of at least three eruptions.

[19] The minimum, maximum, and mean repose time for an eruption sequence is presented along with the minimum and maximum SiO_2 content for the corresponding suite of compositions erupted from a "single" center. Repose time is determined by the interval between the end of one eruption and the start of the next. Measuring repose time is somewhat subjective because what may count as a repose at one volcano may not be considered as a repose elsewhere. Closely observed volcanoes (e.g., Etna or Kilauea) have reposes reported on a scale of days but on older or more silicic volcanoes (e.g., Santorini or St. Helens) have their eruptive periods divided into major eruptive units separated by thousands of years. We have tried to determine repose period as the length of time between eruptions of a characteristic size for that volcano. For example, at Santorini reposes between the Kameni dome-forming eruptions are much shorter than the major ashfall eruptions [*Druitt et al.*, 1999]. This example also highlights the potential for bias

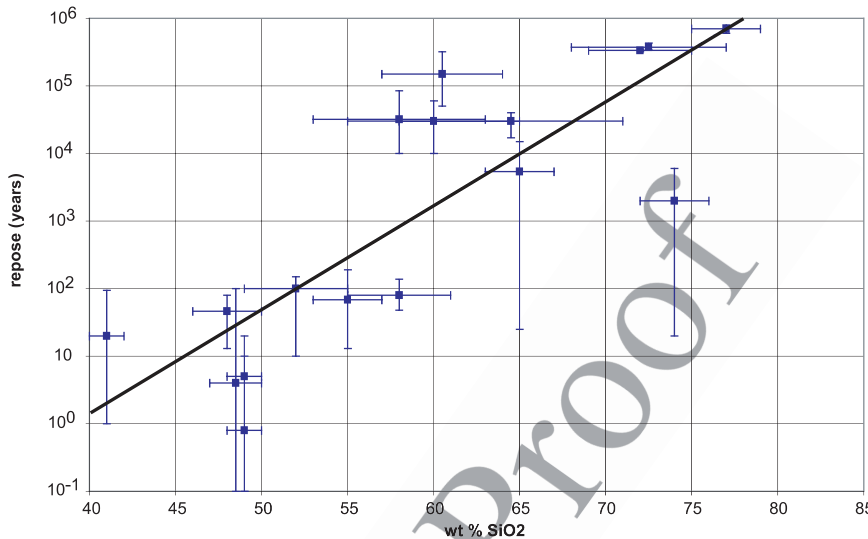

Figure 3. Repose interval between the end of one eruption and the start of the next, and range of SiO_2 content of lavas for locations in Table 4. Error bars represent the high and low values of the data. The points represent the mean repose interval and the middle of the SiO_2 range. The solid line represents the best fit to a least squares regression for an exponential equation which yields $t_{repose} = 10^{-6} * \exp(X/2.78)$. The e-folding factor of 2.78 indicates that repose time increases by a factor of ~3 for each ~3 wt% increase in silica.

toward the Recent with shorter repose times for smaller eruptions that are not preserved in the long-term geologic record. For these reasons, the reposes between major eruptions are considers whereas the "leaking" of minor volumes of lava between major eruptions is not considered in this study.

[20] The exponential relationship between SiO_2 content and repose time is mainly determined by basaltic shields and rhyolite calderas. For volcanoes in the andesite-dacite range, the data jump from short repose intervals to longer repose at ~60% SiO_2 (Figure 3). While composition is unlikely to be the exclusive control on repose time, more error is likely to emerge in the 60–70% SiO_2 range due to difficulties in dating the eruptions of complex stratocones, the dominant constructional volcanic morphology for intermediate compositions. Measuring the repose periods at stratocones and calderas requires high resolution stratigraphy and precise ages over several millennia to smooth out the short-timescale volume/frequency relationship [*Wadge*, 1982]. These data are very limited but are becoming more available recently with improvements in geochronological methods [*Hildreth et al.*, 2003a]. If the maximum SiO_2 in the system controls the repose period then the fit parameter of the exponential equation improves slightly (R^2 = 0.69 to 0.73).

[21] There are several reasons to expect repose time to increase as silica increases. Direct melting of mantle produces basaltic compositions, and more evolved compositions require time for fractional crystallization and assimilation. Higher silica compositions also have greater melt viscosity, requiring additional excess pressure to erupt [*Rubin*, 1995] and, in that sense, are far less mobile. More viscous magmas are more likely to suffer "thermal death" compared to less viscous magmas. A few studies have already pointed out a positive correlation between eruptive volume and repose interval [*Cary et al.*, 1995; *Klein*, 1982; *Wadge*, 1982]. The magma storage time, based on rock geochronometers from crystal ages and from crystal size distribution analysis (CSD), tends to increase exponentially as SiO_2 and stored magma volume increase [*Hawkesworth et al.*, 2004; *Reid*, 2003]. These observations are all consistent with the idea that longer magma storage times allow time for that, in turn, results in longer repose periods associated with higher silica content magmas.

4. Discussion

4.1. Upwelling and Magma Production Rate Limits

[22] Factors that might influence volcanic rates and intrusive:extrusive ratios are local crustal thickness, tectonic setting (magnitude and orientation of principal stresses), magma composition, and melt generation rate in the source region. For 170 examples, long-term volcanic output rate varies

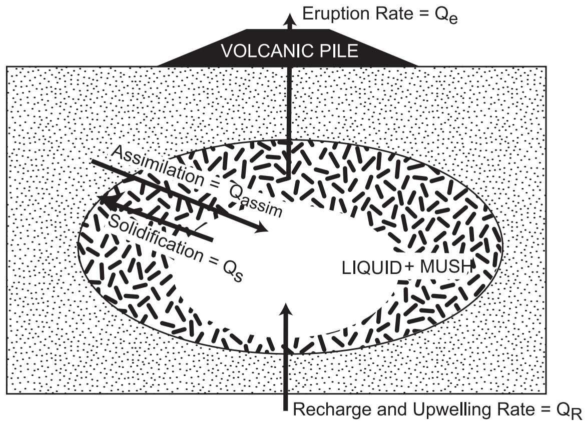

Figure 4. Cartoon of a simplified volcanic system representing storage, and the processes affecting the volume of magma available for eruption. At some depth below the volcano, a volume of magma is stored in a liquid/crystal mush magma chamber. Inputs to the system are by recharge, a function of the magma upwelling rate, and assimilation of host rock. Outputs are by eruption or solidification of the magma by cooling within the magma chamber. A closed volcanic system in this context is one that receives no input.

from 10^{-5} to 1 km^3/yr. Only flood basalts attain the highest Q_e, above 10^{-1} km^3/yr, while various volcanoes with the lowest measured Q_e, below 10^{-5} km^3/yr, seem to have very little in common (Figure 1). Tectonic setting, but not magma composition, affects volcanic rates. Continental crust reduces the average Q_e to 4.4×10^{-3} km^3/yr from 2.8×10^{-2} for oceanic crust.

[23] The output rates all show a strong skewness with long tails toward low Q_e values suggesting that an upper limit may exist (Figure 2). Furthermore, although there is essentially no lower limit to volcanic rates in that magma supplied from depth may intrude but never erupt, or dribble out slowly, this is not usually the case. Most volcanoes have a Q_e above 1×10^{-3} km^3/yr. This result was also found empirically by *Smith* [1979] and *Crisp* [1984]. *Hardee* [1982] derives a simple analytic solution showing that this critical Q_e of $\sim 10^{-3}$ km^3/yr represents a "thermal threshold" where magmatic heat from the intrusion tends to keep a conduit open and begin formation of a magma chamber. We infer that long-term volcanism is unlikely to occur without an open magma conduit to supply and focused melt delivery. This threshold value is dependent on intrusive rate, not volcanic output rate. The I:E ratios found are somewhat lower than the often cited 10:1 ratio, and suggest that an I:E ratio of ~5:1 may be regarded as a better average value. Nevertheless, this suggests that, using the Q_e values present here as data for the *Hardee* [1982] model, virtually all of the volcanic systems in Tables 1 and 2 meet the requirements for conduit wall rock meltback and magma chamber formation.

[24] It is perhaps surprising that given the large differences in eruptive style and melt generation mechanisms (e.g., isentropic decompression, triggering by metasomatic introduction of volatiles or mafic magma underplating) in different tectonic settings an aggregate view of volcanic rates exhibits such a small range of variation, by and large. The similarity of the rates leads us to speculate that a magma upwelling rate limit is set within the mantle at a value near 1 km^3/yr, with magma generation being subject to greater variances based on the local composition of the mantle being melted. In this view, flood basalts represent systems with low I:E ratios and form when a large fraction of mantle-generated magma reaches the surface. The upper limit on magma generation may be controlled by the subsolidus upwelling rate within the upper mantle of 0.01–0.1 m/yr, and this may explain the upper limit of magma generation due to isentropic decompression [*Asimow*, 2002; *Verhoogen*, 1954].

4.2. Openness of Magmatic Systems

[25] The volcanic output rate and repose periods between eruptions gives us some basic constraints on the behavior of magma systems as open or closed systems. We have noted the empirical correlation of repose period and magma silica content. That is, a repose interval can be roughly predicted on the basis of either mean or maximum SiO_2 wt% of the eruptive composition. What constraints can be put on storage time in volcanic systems from purely thermodynamic considerations?

[26] A volcanic system can be crudely modeled as a magma storage zone in the crust and a volcanic pile at the surface (Figure 4). Four processes affect the volume of magma in the storage reservoir or magma chamber: eruption (Q_e) and solidification (Q_s) remove magma from the system, while recharge (Q_R) and crustal assimilation (Q_A) add magma to the system. When a volcano acts as a closed system (one that receives no input of mass or heat via advected hot magma) all of the magma erupted remains molten for the duration of volcanic activity under consideration. In such a system, crystallization can occur due to the loss of heat or volatiles from the magma body to its colder surroundings but the extent of crystallization must

be insufficient to preclude eruption. One way to approach this problem is to assume that volcanoes act as closed systems during repose periods between eruptions and treat each eruption as the result an isolated batch of magma supplied by recharge in a single event and stored until eruption.

[27] Simple heat transfer considerations based on Stefan cooling of magma permit a first-order test of the hypothesis that a volcanic system is a closed system. If we know the eruption rate (Tables 1 and 2), and assume a closed system with respect to mass and heat recharge, the magma in storage will solidify at a rate specified by Stefan cooling. Using data for volcanic output rate of individual eruptions and repose time between eruptions gathered for several volcanic centers at a wide range of eruptive compositions, a simple 1-D Stefan cooling model [*Carslaw and Jaeger*, 1959] can be applied to estimate solidification times t (years) in a spherical magma volume of V (km^3)

$$t = \left(\frac{\sqrt[3]{V}}{2\lambda\sqrt{\kappa}}\right)^2, \tag{1}$$

where κ is the thermal diffusivity, λ is the solution to the transcendental equation

$$L\sqrt{\frac{\pi}{c_p \Delta T}} = \lambda^{-1} erfc \lambda e^{-\lambda^2}, \tag{2}$$

where L is the latent heat of fusion (J kg^{-1}), c_p is the isobaric specific heat capacity (J kg^{-1} K^{-1}), and ΔT is the temperature difference between the ambient external temperature and the liquidus of the melt phase. The thermal diffusivity is calculated as

$$\kappa = K\rho^{-1}c_p^{-1}, \tag{3}$$

where ρ is magma density (kg m^{-3}) and K is magma thermal conductivity (J/kg m s). Values for the various constants are taken from *Spera* [2000] for gabbro, granodiorite, and granite melts. This very basic approach permits a first-order look at the issue of cooling as a constraint on magma system longevity and openness. Heat calculations for lens or sill-like geometries alter the results by a factor of 2–4 [*Fedotov*, 1982]. Consideration of hydrothermal cooling would tend to enhance cooling rates so that the lifetime of a given volume of magma presented here is always an upper limit on cooling times. A more complex model is not justified given the order-of-magnitude estimates used as input.

[28] If we consider that volcanoes act as closed systems only between two successive eruptions, the solution to the 1-D Stefan Problem described above allows us to examine the thermal viability of the volcanic system given the repose period and the volume of magma involved (Figure 5). A closed system, in this context, means that one batch of magma is intruded at some time and stored until the eruption. Thus a maximum "storage time" for a batch of magma in the shallow plumbing system of a volcano can be estimated (Figure 6). The solidification time is determined as the time for a volume of magma to completely solidify as calculated from equation (1). The volume of magma is assumed to be five times the DRE volume of the eruption following the repose period based on the average I:E ratio from the data in Table 3. The assumption of complete solidification puts an upper limit on the time necessary to cool the magma enough to prevent eruption.

[29] Only a handful of volcanoes have been studied well enough to be able to estimate both volume and timing of eruptions over many eruptive cycles. The long, detailed records of eruptions at Mauna Loa [*Klein*, 1982] and Etna [*Tanguy*, 1979; *Wadge*, 1977] are used as examples of basaltic volcanoes, and the regular eruptive pattern at Izu-Oshima for the past 10^3 years [*Koyama and Hayakawa*, 1996; *Nakamura*, 1964] makes the volumes of individual eruptions more clear. Toba [*Chesner and Rose*, 1991] and Yellowstone [*Christiansen*, 2001] are two calderas with a high quality record of multiple major eruptions. A few other examples from volcanoes with shorter, but still well-documented, records are also used with data from sources cited in Table 2.

[30] Whether the magma would solidify, and thus require the volcano to be an open system, depends on the magma storage time. Estimates of magma storage times from various crystal-age geochronometers are available at a range of volcanic centers and suggest that magma storage period, like repose, is a function of silica content of the magma [see *Reid*, 2003, and references therein]. Storage time from crystal ages for basaltic systems are generally longer or equal to repose, while storage times for andesites and rhyolite systems are slightly shorter than or equal to repose. On the basis of this information, we can draw a set of lines for different fractions of storage to repose time representing the limits for volcanoes that may be thermally closed systems between eruptions (Figure 6).

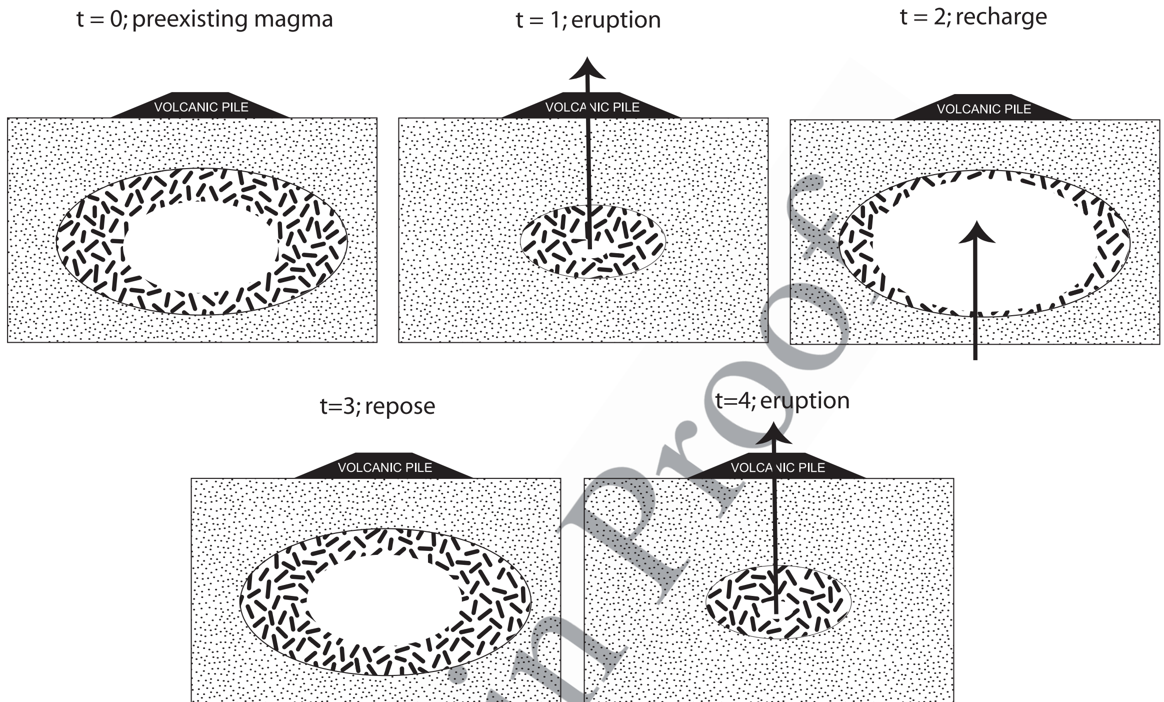

Figure 5. Cartoon depicting a time sequence of a simplified volcano that is closed to mass and advected heat between individual eruptions. The arrows indicate mass inputs and outputs. Eruptible magma is represented by the white oval, the lath pattern is cooling and crystallizing magma, and the stipple is country rock. Time t_0 shows the preexisting conditions, while the sequence begins with the eruption at t_1 which removes the eruptible magma from the magma chamber. Recharge occurs at t_2. Cooling during the storage period, shown in t_3, is the interval between recharge and eruption ($t_2 - t_4$). There must be enough magma left at t_4 to equal the known volume of eruption. The repose period, as calculated for Figure 6, is the interval $t_1 - t_4$. This model assumes that magma is fed into the system in isolated batches, as discussed in the text.

[31] The repose time between eruptions at large calderas (Yellowstone, Long Valley, and Toba) can be more than 10 times greater than the storage time and the volcanoes are still required to be open systems in this analysis (Figure 6). The basaltic systems (Etna, Mauna Loa, and Oshima) are required to be open systems in this analysis only if magma is stored more than 10–100 times longer than the repose period (Figure 6). A few outliers for Etna with extremely short eruption reposes arguably may be the same eruption, but it is easy to see why these might be from "closed" systems on the timescales presented.

4.3. Heat Flux Associated With Magma Transport

[32] Rates of magmatism may be translated into excess heat flows for specific magmatic provinces to obtain estimates of advected heat via magmatism at regional scales over magmatic province timescales. For mafic eruption rate Q_e and an I:E ratio of $\Re$, the volumetric rate of magma flow into the crust is $\Re Q_e$. The excess heat power H (J yr^{-1}) associated with magma transport from mantle to crust is

$$H = \Re \rho Q_e \Delta T \left[c_p + L/\left(T_{liquidus} - T_{solidus}\right)\right], \qquad (4)$$

where ΔT is the temperature difference between the magma and local crust, L is the enthalpy of crystallization (250–400 kJ/kg dependent on magma composition), ρ is magma density, c_p is the isobaric heat capacity of the magma, and $T_{liquidus} - T_{solidus}$ is the liquidus to solidus temperature interval.

[33] As an example, consider the Skye subprovince of the British Tertiary Igneous Province (BTIP). For the estimated volume eruption rate of 2×10^{-3} km^3/yr averaged over ~1600 km^2 area of Skye, the average excess heat flow is ~3.5×10^7 J/m^2/yr (1.1 W/m^2). This excess heat flux is more than an order of magnitude greater than the average terrestrial global heat flux 0.09 W m^{-2}. These estimates are consistent with a crustal thickening rate of ~5 km/My and a background (regional) heat flux

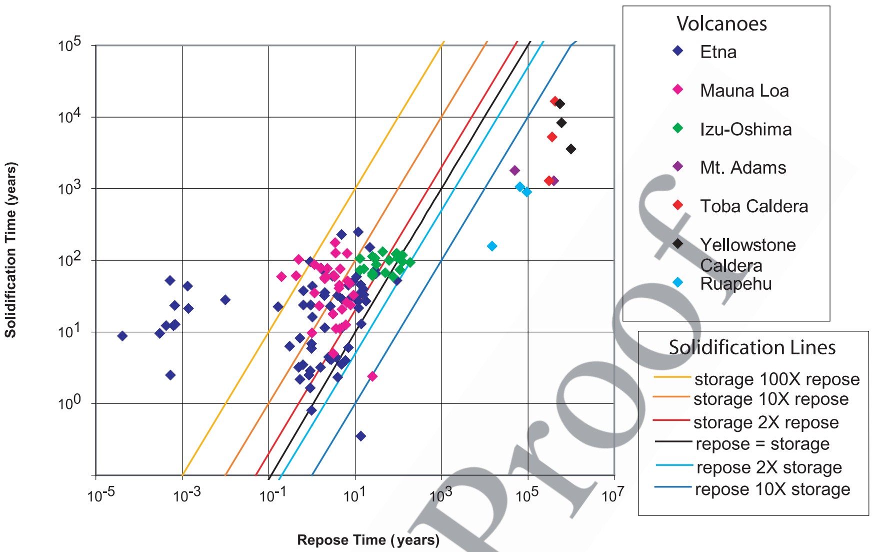

Figure 6. Openness of selected volcanic centers with well-constrained eruptive volumes and repose intervals based on simple 1-D Stefan analysis. Each point, color coded by volcano, represents the repose interval between preceding an eruption and the solidification time for the erupted volume to completely crystallize before erupting. The volume of magma in storage is taken from the intrusive:extrusive ratio in Table 4 or assumed to be 5:1 if unavailable. The colored lines represent cutoff values for the amount of time magma may spend cooling and crystallizing in storage compared to the repose period. Points that plot below the line demand thermodynamically open systems that experience magma recharge prior to eruption. Points above the line may be closed in the sense that multiple eruptions could come from the same batch of magma without additional input. Note that this does not require that these volcanoes act as closed systems.

of 10–15 times the global average during 60–53 Ma. We conclude that the volume flux of magma in the active years of this part of the BTIP focused heat flow about an order of magnitude above the background at the regional scale for ~5 Ma. The regional energy/mass balance estimate appears consistent with inferences drawn from geochemical modeling that point to significant magma recharge during magmatic evolution at Skye [*Fowler et al.*, 2004].

[34] The excess heat power divided by the area affected by volcanism can be compared to the average terrestrial heat flux to the area. The heat power into the crust due to magmatism is therefore approximately 10^{17} J/yr for an overall average eruption rate taken from Table 1 of 10^{-2} km^3/yr for ~1000 km^2 of arc or ridge and I:E ratio of 5. Thus typical values for the "average" magmatic system, 10^1 W/m^2, exceed the global terrestrial background value of 10^{-1} W/m^2 by two orders of magnitude.

5. Conclusions

[35] The 170 long-term estimates of volcanic output rate compiled from literature references from 1962–2004 corroborate much of the previously published information about magmatic systems but also reveal a few surprises. Long-term volcanic rates are higher for basaltic volcanoes than andesitic and rhyolitic volcanoes taken as a group. Oceanic hot spots, arcs, and ridges have an average volcanic output rate of 10^{-2} km^3/yr while continental arcs and hot spots have an average output rate of 10^{-3} km^3/yr, implying that thinner crust/lithosphere is associated with higher volcanic rates on average but not systematically.

[36] For the small number of volcanic systems where adequate data exist (Table 3), the I:E ratio is most commonly less than 10:1 with 2–3:1 being the most commonly occurring value, and a median value of 5:1. On the basis of the data compiled here, there is little indication that composition is strongly or systematically associated with I:E ratio. We conclude only that further work needs to be done on this important topic.

[37] In contrast, composition and repose period between eruptions (end to next start) are strongly linked. We found that an exponential relationship between repose period and silica content of the magma provides a satisfactory fit to the data.

[38] Purely on the basis of thermal considerations, volcanic systems must be open to recharge of magma between individual eruptions, except for the most frequently erupting basaltic volcanoes. The fact that basaltic systems are indeed open magmatic systems can be demonstrated by other means [e.g., *Davidson et al.*, 1988; *Gamble et al.*, 1999; *Hildreth et al.*, 1986].

Acknowledgments

[39] The authors would like to thank Arwen Vidal, Yanhua Anderson, and Joesph Goings for tracking down some of the data that went into the tables. Some of the work that went into this paper was carried out at and for the Jet Propulsion Laboratory, California Institute of Technology, sponsored by the National Aeronautics and Space Administration. Support from NASA, NSF, and the DOE for magma transport research at UCSB is gratefully acknowledged. We thank M. R. Reid, C. R. Bacon, and R. S. J. Sparks for their very thorough and thoughtful reviews.

References

Aguirre-Diaz, G. J., and G. Labarthe-Hernandez (2003), Fissure ignimbrites: Fissure-source origin for voluminous ignimbrites of the Sierra Madre Occidental and its relationship with Basin and Range faulting, *Geology*, *31*(9), 773–776.

Allard, P. (1997), Endogenous magma degassing and storage at Mount Etna, *Geophys. Res. Lett.*, *24*(17), 2219–2222.

Allen, S. R., and I. E. M. Smith (1994), Eruption styles and volcanic hazard in the Auckland Volcanic Field, New Zealand, *Geosci. Rep. Shizuoka Univ.*, *20*, 5–14.

Aranda-Gomez, J. J., J. F. Luhr, T. B. Housh, C. B. Connor, T. Becker, and C. D. Henry (2003), Synextensional Pliocene-Pleistocene eruptive activity in the Camargo volcanic field, Chihuahua, Mexico, *Geol. Soc. Am. Bull.*, *115*, 298–313.

Asimow, P. D. (2002), Steady-state mantle-melt interactions in one dimension; II, Thermal interactions and irreversible terms, *J. Petrol.*, *43*(9), 1707–1724.

Bacon, C. R. (1982), Time-predictable bimodal volcanism in the Coso Range, California, *Geology*, *10*, 65–69.

Bacon, C. R. (1983), Eruptive history of Mount Mazama and Crater Lake Caldera, Cascade Range, U.S.A., *J. Volcanol. Geotherm. Res.*, *18*, 57–115.

Bacon, C. R., and M. Lanphere (1990), The geologic setting of Crater Lake, Oregon, in *Crater Lake: An Ecosystem Study*, edited by E. T. Drake et al., pp. 19–27, Pac. Div. of the Am. Assoc. for the Adv. of Sci., San Francisco, Calif.

Bargar, K. E., and E. D. Jackson (1974), Calculated volumes of individual shield volcanoes along the Hawaiian-Emperor Chain, *J. Res. U. S. Geol. Surv.*, *2*, 545–550.

Becker, K., et al. (1989), Drilling deep into young oceanic crust, Hole 504B, Costa Rica Rift, *Rev. Geophys.*, *27*, 79–102.

Bindeman, I. N., and J. W. Valley (2003), Rapid generation of both high- and low-$\delta^{18}O$, large-volume silicic magmas at the Timber Mountain/Oasis Valley caldera complex, Nevada, *Geol. Soc. Am. Bull.*, *115*(5), 581–595.

Bjarnason, I. T., W. Menke, O. G. Flovenz, and D. Caress (1993), Tomographic image of the Mid-Atlantic plate boundary in southwestern Iceland, *J. Geophys. Res.*, *98*, 6607–6622.

Blatter, D. L., I. S. E. Carmichael, A. L. Deino, and P. R. Renne (2001), Neogene volcanism at the front of the central Mexican volcanic belt: Basaltic andesites to dacites with contemporaneous shosonites and high TiO_2 lava, *Geol. Soc. Am. Bull.*, *113*, 1324–1342.

Bryan, S. E., A. E. Constantine, C. J. Stephens, A. Ewart, R. W. Schon, and J. Parianos (1997), Early Cretaceous volcano-sedimentary successions along the eastern Australia continental margin: Implications for the break-up of eastern Gondwana, *Earth Planet. Sci. Lett.*, *153*, 85–102.

Caress, D. W., M. K. McNutt, R. S. Detrick, and J. C. Mutter (1995), Seismic imaging of hotspot-related crustal underplating beneath the Marquesas Islands, *Nature*, *373*, 600–603.

Carracedo, J. C., S. J. Day, P. Gravestock, and H. Guillou (1999), Later stages of volcanic evolution of La Palma, Canary Islands: Rift evolution, giant landslides, and the genesis of the Caldera de Taburiente, *Geol. Soc. Am. Bull.*, *111*(5), 755–768.

Carrier, D. L., and D. S. Chapman (1981), Gravity and thermal models for the Twin Peaks silicic volcanic center, southwestern Utah, *J. Geophys. Res.*, *86*, 10,287–10,302.

Carslaw, H. S., and J. C. Jaeger (1959), *Conduction of Heat in Solids*, 510 pp., Oxford Univ. Press, New York.

Cary, S., J. Gardner, and H. Sigurdsson (1995), The intensity and magnitude of Holocene plinian eruptions from Mount St. Helens Volcano, *J. Volcanol. Geotherm. Res.*, *66*(1–4), 185–202.

Cawthorn, R. G., and F. Walraven (1998), Emplacement and crystallization time for the Bushveld Complex, *J. Petrol.*, *39*(9), 1669–1687.

Chesner, C. A., and W. I. Rose (1991), Stratigraphy of the Toba Tuffs and the evolution of the Toba Caldera Complex, Sumatra, Indonesia, *Bull. Volcanol.*, *53*, 343–356.

Chevallier, L. (1987), Tectonic and structural evolution of Gough Volcano: A volcanological model, *J. Volcanol. Geotherm. Res.*, *33*, 325–336.

Chiarabba, C., A. Amato, and P. T. Delaney (1997), Crustal structure, evolution, and volcanic unrest of the Alban Hills, central Italy, *Bull. Volcanol.*, *59*, 161–170.

Christiansen, R. L. (2001), The Quaternary and Pliocene Yellowstone Plateau volcanic field of Wyoming, Idaho, and Montana, *U.S. Geol. Surv. Prof. Pap.*, *729*, 1–146.

Christiansen, R. L., and R. H. J. Blank (1972), Volcanic stratigraphy of the Quaternary rhyolite plateau in Yellowstone National Park, in *Geology of Yellowstone National Park*, *U.S. Geol. Surv. Prof. Pap.*, *729-B*, 18 pp.

Clawson, S. R., R. B. Smith, and H. M. Benz (1989), P wave attenuation of the Yellowstone Caldera from three-dimensional inversion of spectral decay using explosion source seismic data, *J. Geophys. Res.*, *94*, 7205–7222.

Condit, C. D., L. S. Crumpler, J. C. Aubele, and W. E. Elston (1989), Patterns of volcanism along the southern margin of the Colorado Plateau: The Springerville field, *J. Geophys. Res.*, *94*(B6), 7975–7986.

Courtillot, V. E., and P. R. Renne (2003), On the ages of flood basalt events, *C. R. Geosci.*, *335*, 113–140.

Crecraft, H. R., W. P. Nash, and S. H. Evans (1981), Late Cenozoic volcanism at Twin Peaks, Utah: Geology and petrology, *J. Geophys. Res.*, *86*, 10,303–10,320.

Crisp, J. A. (1984), Rates of magma emplacement and volcanic output, *J. Volcanol. Geotherm. Res.*, *20*, 177–211.

Criss, R. E., E. B. Ekren, and R. F. Hardyman (1984), Casto Ring Zone: A 4500-km^2 fossil hydrothermal system in the Challis Volcanic Field, central Idaho, *Geology*, *12*, 331–334.

Darbyshire, F. A., I. T. Bjarnason, R. S. White, and O. G. Flovenz (1998), Crustal structure above the Iceland mantle plume imaged by the ICEMELT refraction profile, *Geophys. J. Int.*, *135*, 1131–1149.

Davidson, J. P., K. M. Ferguson, M. T. Colucci, and M. A. Dungan (1988), The origin and evolution of magmas from the San Pedro Pellado volcanic complex, S. Chile; multi-component sources and open system evolution, *Contrib. Mineral. Petrol.*, *100*(4), 429–445.

Davis, J. M., and C. J. Hawkesworth (1995), Geochemical and tectonic transitions in the evolution of the Mogollon-Datil Volcanic Field, New Mexico, USA, *Chem. Geol.*, *119*, 31–53.

de Bremond d'Ars, J., C. Jaupart, and R. S. J. Sparks (1995), Distribution of volcanoes in active margins, *J. Geophys. Res.*, *100*(B10), 20,421–20,432.

Detrick, R. S., A. J. Harding, G. M. Kent, J. A. Orcutt, J. C. Mutter, and P. Buhl (1993), Seismic structure of the southern East Pacific Rise, *Science*, *259*, 499–503.

Doell, R. R., G. B. Dalrymple, R. L. Smith, and R. A. Bailey (1968), Paleomagnetism, potassium-argon ages, and geology of rhyolites and associated rocks of the Valles Caldera, New Mexico, in *Studies in Volcanology*, edited by R. R. Coats, R. L. Hay, and C. A. Anderson, *Mem. Geol. Soc. Am.*, *116*, 211–248.

Doucelance, R., S. Escrig, M. Moreira, C. Gariepy, and M. Kurz (2003), Pb-Sr-He isotope and trace element geochemistry of the Cape Verde Archipelago, *Geochim. Cosmochim. Acta*, *67*, 3717–3733.

Doukas, M. P. (1990), Road guide to volcanic deposits of Mount St. Helens and vicinity, Washington, *U.S. Geol. Surv. Bull.*, *1859*, 53 pp.

Druitt, T. H., L. Edwards, R. M. Mellors, D. M. Pyle, R. S. J. Sparks, M. Lanphere, M. Davies, and B. Barriero (1999), *Santorini Volcano*, *Geol. Soc. London Mem.*, *19*, 176 pp.

Duffield, W. A., C. R. Bacon, and G. B. Dalrymple (1980), Late Cenozoic volcanism, geochronology, and structure of the Coso Range, Inyo County, California, *J. Geophys. Res.*, *85*, 2381–2404.

Duncan, R. A. (1991), Age distribution of volcanism along aseismic ridges in the eastern Indian Ocean, *Proc. Ocean Drill. Program Sci. Results*, *121*, 507–517.

Dungan, M. A., M. M. Lindstrom, N. J. McMillan, S. Moorbath, J. Hoefs, and L. Haskin (1986), Open system magmatic evolution of the Taos Plateau volcanic field, northern New Mexico: 1. The petrology and geochemistry of the Servilleta Basalt, *J. Geophys. Res.*, *91*, 5999–6028.

Dvorak, J. J., and D. Dzurisin (1993), Variations in magma supply rate at Kilauea Volcano, Hawaii, *J. Geophys. Res.*, *98*, 22,255–22,268.

Erlich, E. N., and O. N. Volynets (1979), General problems of petrology and acid volcanism, *Bull. Volcanol.*, *42*, 175–185.

Esser, R. P., P. R. Kyle, and W. C. McIntosh (2004), $^{40}Ar/^{39}Ar$ dating of the eruptive history of Mount Erebus, *Antarctica: Volcano evolution, Bull. Volcanol.*, *66*, 671–686.

Evans, S. H., H. R. Crecraft, and W. P. Nash (1980), K/Ar ages of silicic volcanism in the Twin Peaks/Cove Creek Dome area, southwestern Utah, *Isochron/West*, *28*, 21–24.

Farmer, G. L., D. E. Broxton, R. G. Warren, and W. Pickthorn (1991), Nd, Sr, and O isotopic variations in metaluminous ash-flow tuffs and related volcanic rocks at the Timber Mountains/Oasis Valley caldera complex, SW Nevada: Implications for the origin and evolution of large-volume silicic magma bodies, *Contrib. Mineral. Petrol.*, *109*, 53–68.

Fedotov, S. A. (1982), Temperatures of entering magma, formation and dimensions of magma chambers of volcanoes, *Bull. Volcanol.*, *45*(4), 333–347.

Fitton, J. G., and D. James (1986), Basic volcanism associated with intraplate linear features, *Philos. Trans. R. Soc. London, Ser. A*, *317*, 253–266.

Fowler, S. J., W. A. Bohrson, and F. J. Spera (2004), Magmatic evolution of the Skye Igneous Centre, western Scotland: Modelling of assimilation, recharge, and fractional crystallization, *J. Petrol.*, *45*(12), 2481–2505.

Francis, P. W., and C. J. Hawkesworth (1994), Late Cenozoic rates of magmatic activity in the Central Andes and their relationships to continental crust formation and thickening, *J. Geol. Soc. London, 151*, Part, *5*, 845–854.

Freundt, A. H., and H.-U. Schmincke (1995), Eruption and emplacement of a basaltic welded ignimbrite during caldera formation on Gran Canaria, *Bull. Volcanol.*, *56*, 640–659.

Frey, F. A., et al. (2000), Origin and evolution of a submarine large igneous province: The Kerguelen Plateau and Broken Ridge, southern Indian Ocean, *Earth Planet. Sci. Lett.*, *176*, 73–89.

Frey, H. M., R. A. Lange, C. M. Hall, and H. Delgado-Granados (2004), Magma eruption rates constrained by $^{40}Ar/^{39}Ar$ chronology and GIS for Ceboruco-San Pedro volcanic field, western Mexico, *Geol. Soc. Am. Bull.*, *116*, 259–276.

Gallagher, K., and C. Hawkesworth (1994), Mantle plumes, continental magmatism, and asymmetry in the South Atlantic, *Earth Planet. Sci. Lett.*, *123*, 105–117.

Gamble, J. A., C. P. Wood, R. C. Price, I. E. M. Smith, R. B. Stewart, and T. Waight (1999), A fifty year perspective of magmatic evolution on Ruapehu Volcano, New Zealand; verification of open system behaviour in an arc volcano, *Earth Planet. Sci. Lett.*, *170*, 301–314.

Gamble, J. A., R. C. Price, I. E. M. Smith, W. C. McIntosh, and N. W. Dunbar (2003), $^{40}Ar/^{39}Ar$ geochronology of magmatic activity, magma flux, and hazards at Ruapehu Volcano, Taupo Volcanic Zone, New Zealand, *J. Volcanol. Geotherm. Res.*, *120*, 271–287.

Gerlach, D. C. (1990), Eruption rates and isotopic systematics of ocean islands: Further evidence for small-scale heterogeneity in the upper mantle, *Tectonophysics*, *172*, 273–289.

Greeley, R., and B. D. Schneid (1991), Magma generation on Mars: Amounts, rates, and comparisons with Earth, Moon, and Venus, *Science*, *254*, 996–998.

Grevemeyer, I., E. R. Flueh, C. Reichert, J. Bialas, D. Klaschen, and C. Kopp (2001), Crustal architecture and deep structure of the Ninetyeast Ridge hotspot trail from active-source ocean bottom seismology, *Geophys. J. Int.*, *144*, 414–431.

Guillou, H., J. C. Carracedo, and S. J. Day (1998), Dating of the Upper Pleistocene-Holocene volcanic activity of La Palma using the unspiked K-Ar technique, *J. Volcanol. Geotherm. Res.*, *86*, 137–149.

Haederle, M., and M. Atherton (2002), Shape and intrusion style of the Coastal Batholith, Peru, *Tectonophysics*, *345*, 17–28.

Hall, M. L., C. Robin, B. Beate, P. Mothes, and M. Monzier (1999), Tungurahua Volcano, Ecuador: Structure, eruptive history, and hazards, *J. Volcanol. Geotherm. Res.*, *91*, 1–21.

Hardee, H. C. (1982), Incipient magma chamber formation as a result of repetitive intrusions, *Bull. Volcanol.*, *45*(1), 41–49.

Harding, A. J., J. A. Orcutt, M. E. Kappus, E. E. Vera, J. C. Mutter, P. Buhl, R. S. Detrick, and T. M. Brocher (1989), Structure of young oceanic crust at 13°N on the East Pacific Rise from expanding spread profiles, *J. Geophys. Res.*, *94*, 12,163–12,196.

Harding, A. J., G. M. Kent, and J. A. Orcutt (1993), A multichannel seismic investigation of upper crustal structure at

9°N on the East Pacific Rise: Implications for crustal accretion, *J. Geophys. Res.*, *98*, 13,925–13,944.

Harford, C. L., M. S. Pringle, R. S. J. Sparks, and S. R. Young (2002), The volcanic evolution of Montserrat using $^{40}Ar/^{39}Ar$ geochronology, in *The Eruption of Soufriere Hills Volcano, Montserrat, From 1995 to 1999*, edited by T. H. Druitt and B. P. Kokelaar, *Geol. Soc. London Mem.*, *21*, 93–113.

Hasenaka, T. (1994), Size, distribution, and magma output rate for shield volcanoes of the Michoacan-Guanajuato volcanic field, Central Mexico, *J. Volcanol. Geotherm. Res.*, *63*, 13–31.

Hasenaka, T., and I. S. E. Carmichael (1985), The cinder cones of Michoacan-Guanajuato, Central Mexico: Their age, volume, and distribution, and magma discharge rate, *J. Volcanol. Geotherm. Res.*, *25*, 105–124.

Hawkesworth, C., R. George, S. Turner, and G. Zellmer (2004), Time scales of magmatic processes, *Earth Planet. Sci. Lett.*, *218*, 1–16.

Heiken, G., F. Goff, J. Gardner, and W. Baldridge (1990), The Valles/Toledo Caldera Complex, Jemez Volcanic Field, New Mexico, *Annu. Rev. Earth Planet. Sci.*, *18*, 27–53.

Henry, C. D., M. J. Kunk, and W. C. McIntosh (1994), $^{40}Ar/^{39}Ar$ chronology and volcanology of silicic volcanism in the Davis Mountains, Trans-Pecos Texas, *Geol. Soc. Am. Bull.*, *106*, 1359–1376.

Hildreth, W. (2004), Volcanological perspectives on Long Valley, Mammoth Mountain, and Mono Craters: Several contiguous but discrete systems, *J. Volcanol. Geotherm. Res.*, *136*, 169–198.

Hildreth, W., and J. Fierstein (1997), Recent eruptions of Mount Adams, Washington Cascades, USA, *Bull. Volcanol.*, *58*(6), 472–490.

Hildreth, W., and M. A. Lanphere (1994), Potassium-argon geochronology of a basalt-andesite-dacite arc system: The Mount Adams volcanic field, Cascade Range of southern Washington, *Geol. Soc. Am. Bull.*, *106*, 1413–1429.

Hildreth, W., T. L. Grove, and M. Dungan (1986), Introduction to special section on open magmatic systems, *J. Geophys. Res.*, *91*, 5887–5889.

Hildreth, W., J. Fierstein, and M. Lanphere (2003a), Eruptive history and geochronology of the Mount Baker volcanic field, Washington, *Geol. Soc. Am. Bull.*, *115*(6), 729–764.

Hildreth, W., M. Lanphere, and J. Fierstein (2003b), Geochronology and eruptive history of the Katmai volcanic cluster, Alaska Peninsula, *Earth Planet. Sci. Lett.*, *214*, 93–114.

Hirn, A., A. Nercessian, M. Sapin, F. Ferrucci, and G. Wittlinger (1991), Seismic heterogeneity of Mt Etna: Structure and activity, *Geophys. J. Int.*, *105*, 139–153.

Hobden, B. J., B. F. Houghton, M. Lanphere, and I. A. Nairn (1996), Growth of Tongariro volcanic complex: New evidence from K-Ar age determinations, *N. Z. J. Geol. Geophys.*, *39*(1), 151–154.

Hobden, B. J., B. F. Houghton, J. P. Davidson, and S. P. Weaver (1999), Small and short-lived magma batches at composite volcanoes: Time windows at Tongariro volcano, New Zealand, *J. Geol. Soc. London*, *156*, 865–868.

Hoernle, K., and H.-U. Schmincke (1993a), The role of partial melting in the 15 Ma geochemical evolution of Gran Canaria: A blob model for the Canary Hotspot, *J. Petrol.*, *34*, 599–626.

Hoernle, K., and H.-U. Schmincke (1993b), The petrology of the tholeiites through melilite nephlinites on Gran Canaria, Canary Islands: Crystal fractionation, accumulation, depths of melting, *J. Petrol.*, *34*, 573–597.

Hooft, E. E. E., R. S. Detrick, D. R. Toomey, J. A. Collins, and J. Lin (2000), Crustal thickness and structure along three contrasting spreading segments of the Mid-Atlantic Ridge, 33.5°–35°N, *J. Geophys. Res.*, *105*, 8205–8226.

Johnson, J. S., S. A. Gibson, R. N. Thompson, and G. M. Nowell (2005), Volcanism in the Vitim volcanic field, Siberia: Geochemical evidence for a mantle plume beneath the Baikal Rift Zone, *J. Petrol.*, *46*(7), 1309–1344.

Jourdan, F., G. Feraud, H. Bertand, A. Kampunzu, G. Tshoso, M. Watkeys, and B. LeGall (2005), Karoo large igneous province: Brevity, origin, and relation to mass extinction questioned by new $^{40}Ar/^{39}Ar$ age data, *Geology*, *33*, 745–748.

Kamata, H., and T. Kobayashi (1997), The eruptive rate and history of Kuju Volcano in Japan during the past 15,000 years, *J. Volcanol. Geotherm. Res.*, *76*(1–2), 163–171.

Kaneoka, I., H. Mehnert, S. Zashu, and S. Kawachi (1980), Pleistocene volcanic activities in the Fossa Magna region, central Japan: K-Ar studies of the Yatsugatake volcanic chain, *Geochem. J.*, *14*, 249–257.

Karson, J. A. (1998), Internal structure of oceanic lithosphere: A perspective from tectonic windows, in *Faulting and Magmatism at Mid-ocean Ridges*, *Geophys. Monogr. Ser.*, vol. 106, edited by W. R. Buck et al., pp. 177–218, AGU, Washington, D. C.

Karson, J. A. (2002), Geologic structure of the uppermost oceanic crust created at fast- to intermediate-rate spreading centers, *Annu. Rev. Earth Planet. Sci.*, *30*, 347–384.

Kay, S. M., and R. W. Kay (1985), Role of crystal cumulates and the oceanic crust in the formation of the lower crust of the Aleutian arc, *Geology*, *13*, 461–464.

Klein, F. W. (1982), Patterns of historical eruptions at Hawaiian volcanoes, *J. Volcanol. Geotherm. Res.*, *12*, 1–35.

Koyama, M., and Y. Hayakawa (1996), Syn- and post-caldera eruptive history of Izu Oshima Volcano based on tephra and loess stratigraphy, *J. Geogr.*, *105*, 133–162.

Kumagai, H., T. Ohminato, M. Nakano, M. Ooi, A. Kubo, H. Inoue, and J. Oikawa (2001), Very-long-period seismic signals and caldera formation at Miyake Island, Japan, *Science*, *293*, 687–690.

Kuntz, M. A., D. E. Champion, E. C. Spiker, and R. H. Lefebvre (1986), Contrasting magma types and steady-state, volume-predictable basaltic volcanism along the Great Rift, Idaho, *Geol. Soc. Am. Bull.*, *97*, 579–594.

Larsen, G. (2000), Holocene eruptions within the Katla volcanic system, South Iceland: Characteristics and environmental impact, *Joekull*, *49*, 1–28.

Lewis-Kenedi, C. B., R. A. Lange, C. M. Hall, and H. Delgado-Granados (2005), The eruptive history of Tequila volcanic field, western Mexico: Ages, volumes, and relative proportions of lava types, *Bull. Volcanol.*, *67*, 391–414.

Lipman, P. W. (1984), The roots of ash-flow calderas in western North America: Windows into the tops of granitic batholiths, *J. Geophys. Res.*, *89*, 8801–8841.

Lipman, P. W. (1995), Declining growth of Mauna Loa during the last 100,000 years: Rates of lava accumulation vs. gravitational subsidence, in *Mauna Loa Revealed: Structure, Composition, History, and Hazards*, *Geophys. Monogr. Ser.*, vol. 92, edited by J. M. Rhodes and J. P. Lockwood, pp. 45–80, AGU, Washington, D. C.

Luhr, J. F. (2000), The geology and petrology of Volcan San Juan (Nayrit, Mexico) and the compositionally zoned Tepic Pumice, *J. Volcanol. Geotherm. Res.*, *95*, 109–156.

Luhr, J. F., and I. S. E. Carmichael (1980), The Colima Volcanic Complex, Mexico, *Contrib. Mineral. Petrol.*, *71*, 343–372.

Marsh, B. D. (1989), Magma chambers, *Annu. Rev. Earth Planet. Sci.*, *17*, 439–474.

Martin, D. P., and W. I. Rose (1981), Behavioral patterns of Fuego Volcano, Guatemala, *J. Volcanol. Geotherm. Res.*, *10*, 67–81.

Marzoli, A., E. M. Piccirillo, P. R. Renne, G. Belleini, M. Iacumin, J. B. Nyobe, and A. T. Tongwa (2000), The Cameroon Line revisited: Petrogenesis of continental basaltic magmas from lithospheric and asthenospheric sources, *J. Petrol.*, *41*, 87–109.

Maund, J. G., D. C. Rex, A. P. Leroex, and D. L. Reid (1988), Volcanism on Gough Island: A revised stratigraphy, *Geol. Mag.*, *125*(2), 175–181.

McConnell, V. S., C. K. Shearer, J. C. Eichelberger, M. J. Keskinen, P. W. Layer, and J. J. Papike (1995), Rhyolite intrusions in the intracaldera Bishop Tuff, Long Valley Caldera, California, *J. Volcanol. Geotherm. Res.*, *67*, 41–60.

Menke, W., M. West, B. Brandsdottir, and D. Sparks (1998), Compressional and shear velocity structure of the lithosphere in northern Iceland, *Bull. Seismol. Soc. Am.*, *88*, 1561–1571.

Mertes, H., and H.-U. Schmincke (1985), Mafic postassic lavas of the Quaternary West Eifel volcanic field, I. major and trace elements, *Contrib. Mineral. Petrol.*, *89*, 330–345.

Miller, D. S., and R. B. Smith (1999), P and S velocity structure of the Yellowstone volcanic field from local earthquake and controlled-source tomography, *J. Geophys. Res.*, *104*, 15,105–15,121.

Mori, J., D. Eberhart-Phillips, and D. H. Harlow (1996), Three-dimensional velocity structure at Mount Pinatubo: Resolving magma bodies, in *Fire and Mud: Eruptions and Lahars of Mount Pinatubo, Philippines*, edited by C. G. Newhall and R. S. Punongbayan, pp. 371–385, U.S. Geol. Surv., Seattle, Wash.

Moyer, T. C., and S. Esperanca (1989), Geochemical and isotopic variations in a bimodal magma system: The Kaiser Spring Volcanic Field, Arizona, *J. Geophys. Res.*, *94*(B6), 7841–7859.

Mullineaux, D. R. (1996), Pre-1980 tephra-fall deposits erupted from Mount St. Helens, Washington, *U.S. Geol. Surv. Prof. Pap.*, *1563*.

Nakamura, K. (1964), Volcano-stratigraphic study of Oshima volcano, Izu, *Bull. Earthquake Res. Inst. Tokyo*, *42*, 649–728.

Neal, C. R., J. J. Mahoney, L. Kroenke, R. A. Duncan, and M. G. Petterson (1997), The Ontong Java Plateau, in *Large Igneous Provinces: Continental, Oceanic, and Planetary Flood Volcanism*, *Geophys. Monogr. Ser.*, vol. 100, edited by J. J. Mahoney and M. F. Coffin, pp. 183–216, AGU, Washington, D. C.

Nicolaysen, K., F. A. Frey, K. V. Hodges, D. Weis, and A. Giret (2000), $^{40}Ar/^{39}Ar$ geochronology of flood basalts from the Kerguelen Archipelago, southern Indian Ocean: Implications for Cenozoic eruption rates of the Kerguelen plume, *Earth Planet. Sci. Lett.*, *174*, 313–328.

Nielsen, R. L., and M. A. Dungan (1985), The petrology and geochemistry of Ocate volcanic field, north-central New Mexico, *Geol. Soc. Am. Bull.*, *96*, 296–312.

Nielson, D. L., and B. S. Sibbett (1996), Geology of Ascension Island, South Atlantic Ocean, *Geothermics*, *25*(4–5), 427–448.

Oishi, M., and T. Suzuki (2004), Tephrostratigraphy and eruptive history of the Younger Tephra Beds from the Yatsugatake Volcano, Central Japan, *Bull. Volcanol. Soc. Jpn.*, *49*(1), 1–12.

Olson, P. (1994), Mechanics of flood basalt magmatism, in *Magmatic Systems*, edited by M. P. Ryan, pp. 1–18, Elsevier, New York.

Oversby, V. M., and P. W. Gast (1970), Isotopic composition of lead from oceanic islands, *J. Geophys. Res.*, *75*, 2097–2114.

Pankhurst, R. J., P. T. Leat, P. Sruoga, C. W. Rapela, M. Marquez, B. C. Storey, and T. R. Riley (1998), The Chon Aike Province of Patagonia and related rocks in West Antarctica: A large silicic igneous province, *J. Volcanol. Geotherm. Res.*, *81*, 113–136.

Paris, R., H. Guillou, J. C. Carracedo, and F. J. Perez-Torrado (2005), Volcanic and morphological evolution of La Gomera (Canary Islands), based on new K-Ar ages and magnetic stratigraphy: Implications for ocean island evolution, *J. Geol. Soc. London*, *162*, 501–512.

Patino, L. C., M. J. Carr, and M. D. Feigenson (2000), Local and regional variations in Central American arc lavas controlled by variations in subducted sediment input, *Contrib. Mineral. Petrol.*, *138*, 265–283.

Perry, F. V., B. M. Crowe, G. A. Valentine, and L. M. Bowker (1998), Volcanism studies: Final report for the Yucca Mountain Project, Los Alamos Natl. Lab., Los Alamos, N. M.

Petford, N., and K. Gallagher (2001), Partial melting of mafic (amphibolitic) lower crust by periodic influx of basaltic magma, *Earth Planet. Sci. Lett.*, *193*, 483–499.

Plesner, S., P. M. Holm, and J. R. Wilson (2002), ^{40}Ar-^{39}Ar geochronology of Santo Antao, Cape Verde Islands, *J. Volcanol. Geotherm. Res.*, *120*, 103–121.

Quane, S. L., M. O. Garcia, H. Guillou, and T. P. Hulsebosch (2000), Magmatic history of the East Rift Zone of Kilauea Volcano, Hawaii based on drill core from SOH1, *J. Volcanol. Geotherm. Res.*, *102*, 319–338.

Reid, M. R. (2003), Timescales of magma transfer and storage in the crust, in *Treatise on Geochemistry*, pp. 167–193, Elsevier, New York.

Reidel, S. P., T. L. Tolan, P. R. Hooper, M. H. Beeson, K. R. Fecht, R. D. Bentley, and J. L. Anderson (1989), The Grande Ronde Basalt, Columbia River Basalt Group: Stratigraphic descriptions and correlations in Washington, Oregon, and Idaho, *Spec. Pap. Geol. Soc. Am.*, *239*, 21–53.

Renne, P. R., and A. R. Basu (1991), Rapid eruption of the Siberian Traps flood basalts at the Permo-Triassic boundary, *Science*, *253*(5016), 176–179.

Riehle, J. R., D. A. Champion, and M. A. Lanphere (1992), Pyroclastic deposits of Mount Edgecumbe Volcanic Field, Southeast Alaska, *J. Volcanol. Geotherm. Res.*, *53*(1–4), 117–143.

Riisager, P., J. Riisager, N. Abrahamsen, and R. Waagstein (2002), New paleomagnetic pole and magnetostratigraphy of Faroe Islands flood volcanics, North Atlantic Igneous Province, *Earth Planet. Sci. Lett.*, *201*(2), 261–276.

Rubin, A. M. (1995), Propagation of magma-filled cracks, *Annu. Rev. Earth Planet. Sci.*, *23*, 287–336.

Schweitzer, J. K., C. J. Hatton, and S. A. De Waal (1997), Link between the granitic and volcanic rocks of the Bushveld Complex, South Africa, *J. African Earth Sci.*, *24*(12), 95–104.

Shaw, H. R. (1980), The fracture mechanisms of magma transport from the mantle to the surface, in *Physics of Magmatic Processes*, pp. 201–264, Princeton Univ. Press, Princeton, N. J.

Shaw, H. (1985), Links between magma-tectonic rate balances, plutonism, and volcanism, *J. Geophys. Res.*, *90*, 11,275–11,288.

Shaw, H. R., E. D. Jackson, and K. E. Bargar (1980), Volcanic periodicity along the Hawaiian-Emperor Chain, *Am. J. Science*, *280-A*, 667–708.

Sherrod, D. R., and J. G. Smith (1990), Quaternary extrusion rates of the Cascade Range, northwestern United States and southern British Columbia, *J. Geophys. Res.*, *95*(B12), 19,465–19,474.

Singer, B., R. Thompson, M. Dungan, T. Feely, S. Nelson, J. Pickens, L. Brown, A. Wulff, J. Davidson, and J. Metzger (1997), Volcanism and erosion during the past 930 k. y. at the Tartara-San Pedro complex, Chilean Andes, *Geol. Soc. Am. Bull.*, *109*, 127–142.

Singer, B. S., J. D. Myers, and C. D. Frost (1992), Mid-Pleistocene lavas from the Seguam Island volcanic center, central Aleutian arc: Closed-system fractional crystallization of a basalt to rhyodacite eruptive suite, *Contrib. Mineral. Petrol.*, *110*, 87–112.

Sinton, C. W., R. A. Duncan, B. C. Storey, J. Lewis, and J. Estrada (1998), An oceanic flood basalt province within the Caribbean plate, *Earth Planet. Sci. Lett.*, *155*, 221–235.

Smith, R. L. (1979), Ash-flow magmatism, *Spec. Pap. Geol. Soc. Am.*, *180*, 5–27.

Spera, F. J. (2000), Physical properties of magmas, in *Encyclopedia of Volcanoes*, edited by H. Sigurdsson, pp. 171–190, Elsevier, New York.

Spera, F. J., D. A. Yuen, and S. J. Kirschvink (1982), Thermal boundary layer convection in silicic magma chambers: Effects of temperature-dependent rheology and implications for thermogravitational chemical fractionation, *J. Geophys. Res.*, *87*, 8755–8767.

Staples, R. K., R. S. White, B. Brandsdottir, W. Menke, P. K. H. Maguire, and J. H. McBride (1997), Faroe-Iceland Ridge Experiment: 1. Crustal structure of northeastern Iceland, *J. Geophys. Res.*, *102*, 7849–7866.

Stewart, K., S. Turner, S. Kelley, C. Hawkesworth, L. Kirstein, and M. Mantovani (1996), 3-D, Ar-Ar geochronology in the Parana continental flood basalt province, *Earth Planet. Sci. Lett.*, *143*, 95–109.

Sutton, A. N., S. Blake, C. J. N. Wilson, and B. L. Charlier (2000), Late Quaternary evolution of a hyperactive rhyolite magma system: Taupo volcanic centre, New Zealand, *J. Geophys. Soc. London*, *157*, Part 3, 537–552.

Svensen, H., S. Planke, A. Malthe-Sorenssen, B. Jamtveit, R. Myklebust, T. R. Eidem, and S. Rey (2004), Release of methane from a volcanic basin as a mechanism for initial Eocene global warming, *Nature*, *429*, 542–545.

Tanaka, K. L., E. M. Shoemaker, G. E. Ulrich, and E. W. Wolfe (1986), Migration of volcanism in the San Francisco volcanic field, Arizona, *Geol. Soc. Am. Bull.*, *97*(2), 129–141.

Tanguy, J. C. (1979), The storage and release of magma on Mount Etna: A discussion, *J. Volcanol. Geotherm. Res.*, *6*, 179–188.

Thorarinsson, S., and G. E. Sigvaldason (1972), The Hekla eruption of 1970, *Bull. Volcanol.*, *36*, 269–288.

Thouret, J.-C., A. Finizola, M. Fornari, A. Legeley-Padovani, J. Suni, and M. Frechen (2001), Geology of El Misti volcano near the city of Arequipa, Peru, *Geol. Soc. Am. Bull.*, *113*, 1593–1610.

Togashi, S., N. Miyaji, and H. Yamazaki (1991), Fractional crystallization in a large tholeiitic magma chamber during the early stage of Younger Fuji Volcano, *Bull. Volcanol. Soc. Japan*, *36*, 269–280.

Tolan, T. L., S. P. Reidel, M. H. Beeson, J. L. Anderson, K. R. Fecht, and D. A. Swanson (1989), Revisions to the estimates of the areal extent and volume of the Columbia River Basalt Group, *Spec. Pap. Geol. Soc. Am.*, *239*, 1–20.

Tolstoy, M., A. J. Harding, and J. A. Orcutt (1993), Crustal thickness on the Mid-Atlantic Ridge: Bull's-eye gravity anomalies and focused accretion, *Science*, *262*(5134), 726–729.

Trusdell, F. A., R. B. Moore, V. Carvalho-Martins, and A. Querido (1995), The eruption of Fogo Volcano, Cape Verde Islands, April–May, 1995, *Eos Trans. AGU*, *76*(46), Fall Meet. Suppl., F681.

Tucholke, B. E., J. Lin, M. C. Kleinrock, M. A. Tivey, T. B. Reed, J. Goff, and G. E. Jaroslow (1997), Segmentation and crustal structure of the western Mid-Atlantic Ridge flank, 25°25′–27°10′N and 0–29 m.y., *J. Geophys. Res.*, *102*(B5), 10,203–10,224.

Twist, D., and B. M. French (1983), Voluminous acid volcanism in the Busheveld Complex: A review of the Rooiberg Felsite, *Bull. Volcanol.*, *46*, 225–242.

Verhoogen, J. (1954), Petrological evidence on temperature distribution in the mantle of the Earth, *Eos Trans. AGU*, *35*, 85–92.

Vidal, V., and A. Bonneville (2004), Variations of the Hawaiian hot spot activity revealed by variations in the magma production rate, *J. Geophys. Res.*, *109*, B03104, doi:10.1029/2003JB002559.

Wadge, G. (1977), The storage and release of magma on Mount Etna, *J. Volcanol. Geotherm. Res.*, *2*, 361–384.

Wadge, G. (1980), Output rate of magma from active central volcanoes, *Nature*, *288*, 253–255.

Wadge, G. (1982), Steady state volcanism: Evidence from eruption histories of polygenetic volcanoes, *J. Geophys. Res.*, *87*, 4035–4049.

Wadge, G. (1984), Comparison of volcanic production rates and subduction rates in the Lesser Antillies and Central America, *Geology*, *12*, 555–558.

Walker, G. P. L. (1993), Basaltic-volcano systems, in *Magmatic Processes and Plate Tectonics*, *Geol. Soc. Spec. Publ.*, *76*, 3–38.

Weiland, C. M., L. K. Steck, P. B. Dawson, and V. A. Korneev (1995), Nonlinear teleseismic tomography at Long Valley caldera, using three-dimensional minimum travel time ray tracing, *J. Geophys. Res.*, *100*, 20,379–20,390.

Wolfe, E. W., and R. P. Hoblitt (1996), Overview of the eruptions, in *Fire and Mud: Eruptions and Lahars of Mount Pinatubo, Philippines*, edited by C. G. Newhall and R. S. Punongbayan, pp. 3–20, U.S. Geol. Surv., Seattle, Wash.

Zielinski, R. A., and F. A. Frey (1970), Gough Island: Evaluation of a fractional crystallization model, *Contrib. Mineral. Petrol.*, *29*, 242–254.